Full paper / Mémoire

Study of an anti-poisoning catalyst for methanol electro-oxidation based on PAn−C composite carriers

Yiting Xu, Xiaoliang Peng, Haitao Zeng, Lizong Dai[*], Huihuang Wu

State Key Laboratory for Physical Chemistry of Solid Surfaces and Department of Materials Science and Engineering, College of Chemistry and Chemical Engineering, Xiamen University, Xiamen, Fujian, 361005, PR China

Abstract

The polyaniline−XC-72R carbon composites (PAn−C) are synthesized by in-situ chemical polymerization at low temperature. As a catalyst carrier we deposited platinum on the composite using chemical deposition. The conformation of carriers and catalysts is studied by SEM and FTIR. Methanol oxidation on the catalyst-modified electrode has been measured by cyclic voltammetry (CV) in comparison with the traditional Pt/C focusing on the attenuation of current in a period of time. It is proved that the CO anti-poisoning ability increase may be due to the synergistic effects between the carrier and the catalyst. We get the result that when the mass ratio of PAn to C is 0.25 in composite, the onset potential is the lowest, which indicates the best catalysis. Measured by XRD and SEM, it indicated that the size of Pt particles was decreased and that the dispersion is better when PAn exists in the composite carriers. *To cite this article: Y. Xu et al., C. R. Chimie 11 (2008).*
© 2007 Published by Elsevier Masson SAS on behalf of Académie des sciences.

Keywords: Polyaniline; In-situ polymerization; Methanol oxidation; CO poisoning

1. Introduction

The studies on alcohol electro-oxidation have provided more and more developmental changes for fuel cell [1−3]. Platinum is the most suitable catalyst for direct methanol fuel cell (DMFC), but there are also some difficulties for it, such as low rate of methanol electro-oxidation due to low utilization of Pt and Pt poisoning. In order to increase the anti-poisoning ability of a Pt catalyst, many ways have been reported. One of the important ways is adopting Pt-alloy technology to reduce CO oxidizing potential, including binary and ternary alloys,

such as Pt−Ru, Pt−Sn, Pt−Ru−Mo, Pt−Ru−W, Pt−Ru−Os, Pt−WO3. Another one is the synthesis of metal−organic macrocyclic chelate catalyst without Pt. Preparation of composite catalyst with conducting polymer and development of new carbon support materials as carrier were also reported. The anti-poisoning abilities of CPs have been reported in many references [4−6]. The main carbon materials reported are Vulcan XC-72 carbon, carbon nano-tubes (CNTs), graphite carbon nano-fibres (GCNFs), mesocarbon microbead [7,8]. Conducting polymers as catalyst carriers for DMFC, such as polyaniline (PAn), polythiophene (PTh), polypyrrole (PPy), and so on, are among the most attractive subjects [9−14]. But their low conductivity compared to carbon and their stability during catalyst working

* Corresponding author.
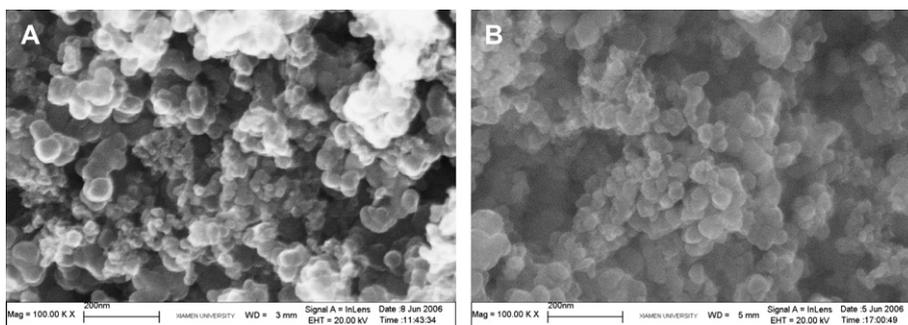*E-mail address:* lzdai@xmu.edu.cn (L. Dai).

Fig. 1. SEM micrographs of XC-72R carbon powder. A: un-treated Vulcan XC-72R carbon; B: Vulcan XC-72R carbon pretreated by HNO₃.

are problems for conducting polymers as platinum carriers.

Along with the development of composites, more and more attention has been paid to conducting polymer composites. But use of the materials as catalyst carriers for DMFC is scarce [15,16]. In this paper, we prepared conducting polymer and carbon composite by in-situ method, and platinized it, obtaining a composite catalyst in order to enhance Pt catalyst anti-poisoning ability, and prolong the catalyst's operating life.

2. Experimental

2.1. Preparation of PAn–C composite carriers

XC-72R carbon was pretreated by boiling in a 4 mol/L HNO₃ solution for 4 h, then washed with de-ionized

water until pH = 7. After the pretreated carbon was dispersed in 1 mol/L H₂SO₄ solution by ultrasonic oscillator, aniline (An) was added into the solution under magnetic stirring. After 30 min, polymerization was initiated by the addition of ammonium persulfate (APS) dropwise. The APS amount was such as [An]:[APS] = 1:1. The reaction mixture was stirred for 2 h. The PAn–C composite precipitate was filtered off and washed with de-ionized water until pH = 7, then with methanol to remove oligomers until the filtrate became colourless. The powder was dried in a vacuum oven at 70 °C.

2.2. Platinized PAn–C and C carriers

PAn–C composite (0.1 g) or XC-72 carbon was mixed with a 1.65 mL H₂PtCl₆ solution (0.077 mol/L) in pH = 4 acetic acid buffer solution in an ultrasonic
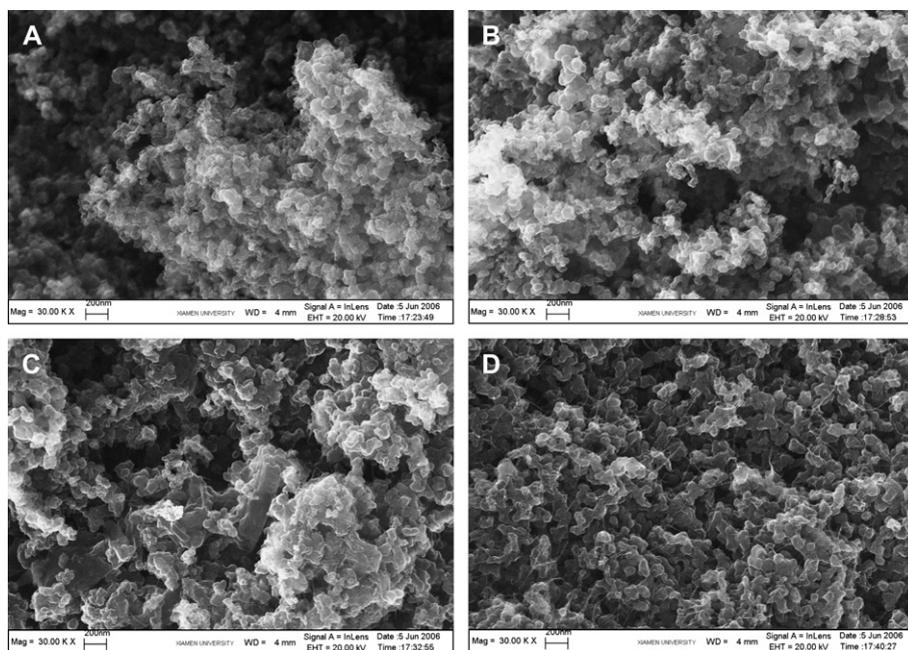

Fig. 2. SEM micrographs of PAn and carbon composite. A: 0.125:1 PAn–C; B: 0.25:1 PAn–C; C: 0.5:1 PAn–C; D: 0.75:1 PAn–C.
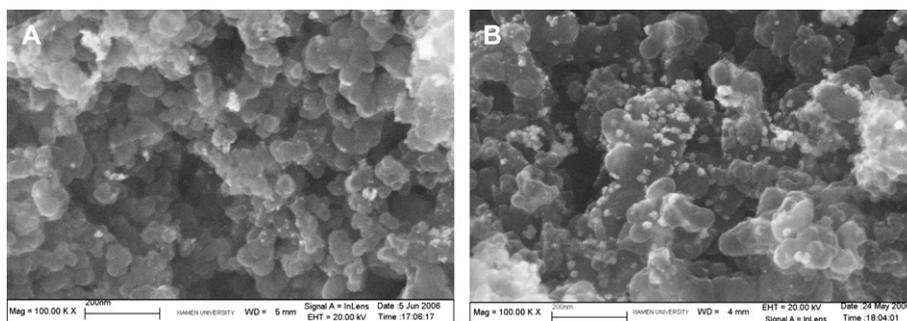
Fig. 3. SEM micrograph of the platinized carriers. A: Pt/C; B: Pt/0.25:1 PAn–C.

oscillator. After 30 min, excess sodium borohydride solution was added. The reaction mixture was stirred for 2 h. The platinized products were filtered off and washed with de-ionized water until no Cl^- was found. The black powder was dried in a vacuum oven at 80 °C. They were labeled as Pt/PAn–C or Pt/C.

2.3. Carriers and catalyst characterization

The FTIR spectra of the samples were recorded with a Nicolet Avatar 360 Fourier infrared spectrophotometer (FTIR) with the KBr pellet technique. Scanning electron measurements (SEM) were performed with a LEO 1530 (Oxford Instrument, England). Measurements of X-ray diffraction spectra were performed on a Panalytical X′Pert diffractometer (Philips, Holland).

2.4. Catalyst-modified electrode preparation

The GC electrode ($d = 5$ mm) was polished to obtain a minute surface, then ultrasonically washed in de-ionized water for 5 min, then in a 5 mol/L HNO_3 solution for 5 min. At the end, the GC electrode was washed

Fig. 4. XRD pattern of Pt/C and Pt/0.25:1 PAn–C.

with water. The prepared catalyst was mixed with iso-propanol, 5% PTFE emulsion, and de-ionized water in ultrasonic oscillator to obtain an ink-like solution. The catalyst-modified electrode was prepared by adding the solution on a GC electrode, and drying it under infra-red light. The platinized amount is about 0.5 mg/cm^2.

2.5. Electrochemical experiments

Voltammetric experiments were performed with an EG&G 263 electrochemical workstation. A three-electrode cell was used with a saturated calomel reference electrode (SCE) and a platinum counter electrode. The catalyst-modified electrodes were used as working electrodes. In all experiments, the scan rate is the same, 50 mV/s.

3. Results and discussion

3.1. Analysis of structure and morphology of catalysts and carriers

Fig. 1 displays the SEM photos of XC-72R carbon. The original carbon appears as agglomerated particles because of the impurities. But after the carbon was pre-treated by HNO_3, it becomes dispersed evenly. In FTIR spectra, the peak of 1600 cm^{-1} is related to aromatic rings, reflecting the basic structural feature of carbon. The peak at 1230 cm^{-1} is attributed to the oxygen-containing group (−C−O−) on the carbon surface. And the peak strength increases after pretreatment by HNO_3, and the carbonyl peak also appears at 1730 cm^{-1}. More oxygen-containing group (−OH, and −COOH, etc.) will help to improve carbon surface wet-tability. During the platinization process, it will promote Pt precursor absorption on carbon surface equally, which is useful to form highly dispersive Pt particles [17].

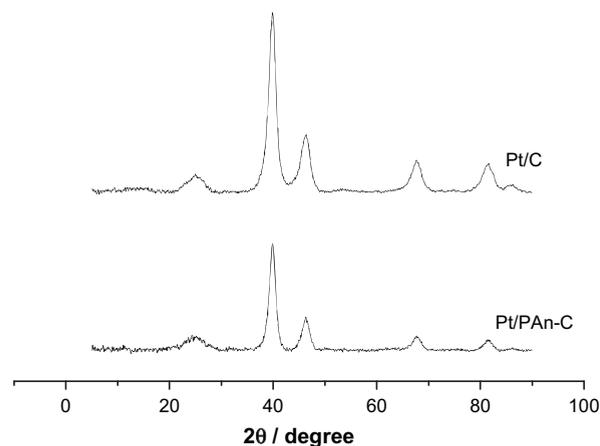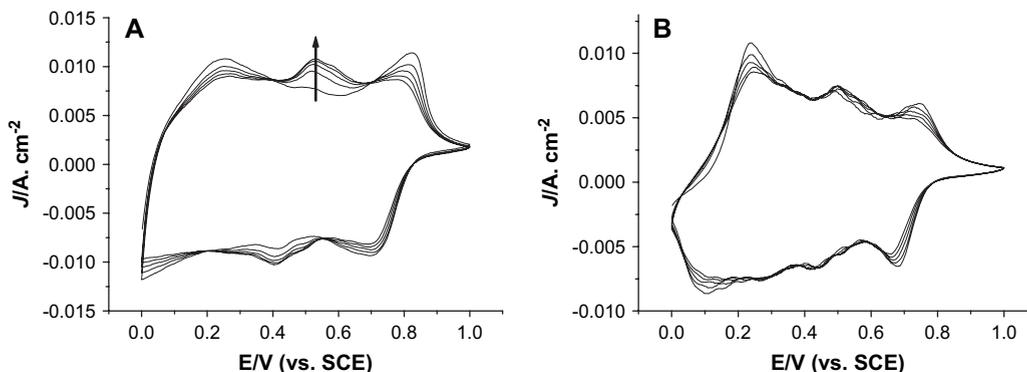After XC-72 carbon compound synthesis with PAn by in-situ chemical polymerization, FTIR spectra of

Fig. 5. CV curves of different modified electrode in 1.0 mol/L H$_2$SO$_4$ (scan rate: 50 mV/s). A: 0.25:1 PAn–C; B: Pt/0.25:1 PAn–C.

the composites indicate that the existence of carbon does not affect the chain structure of PAn. Fig. 2 displays the SEM photos of a PAn–C composite with different mass ratios of PAn to carbon. When the ratio is 0.125:1 or 0.25:1, polymer particles absorb on the carbon particles, and the sizes of the two kinds of particles are similar. It is difficult to distinguish PAn from C particles. If the ratio is higher, the polymer shows larger particles and blocks dispersing in carbon particles, and when PAn:C = 0.75:1, besides some PAn particles, there are also some nano-wires linked to them. Controlling an optimal ratio of PAn to C is the key work to prepare suitable composite carriers. More PAn will decrease the conductivity of composite, whereas too little PAn is not useful because introducing PAn into composite improves the catalyst's anti-poisoning ability.

Fig. 3 displays the SEM photos for platinized XC-72 carbon and PAn–C composite by chemical deposition. Pt particles on carbon carriers scatter sparsely, and agglomerate locally. When the carbon is modified by PAn, Pt particles are evenly distributed, and the average grain size of Pt particle is about 8 nm.

Fig. 4 displays the XRD spectra of platinized XC-72 carbon and PAn–C composite. The peaks at 39.9°, 46.5°, 67.8°, 81.2° correspond to the [111], [200], [220], [311] crystal planes of Pt. According to the half-peak breadth of the strongest peak, Pt[111], the platinum grain size can be calculated by the Scherrer formula. In composite carriers, the size is 7.54 nm, less than that in the carbon carrier, 10.89 nm. The smaller size will provide the Pt particle with a larger specific surface and will raise its catalytic ability.

3.2. Electrochemical study of the composite catalyst

Figs. 5A and B display the CV spectra of the PAn–C composite and the Pt/PAn–C catalyst, respectively. The

shape of their curves is similar, all with two pairs of redox peaks. The reduced leucoemeraldine-to-intermediate-emeraldine transition potential is near 0.2 V and the intermediate emeraldine-to-fully-oxidized-pernigraniline transition potential is 0.8 V. Moreover, there is a new pair of redox peaks appearing in 0.5 V, caused by the degradation products of PAn [18]. In Fig. 6A, the peak current increases with the number of cycles. But after the composite is platinized, the peak current does not change evidently (Fig. 6B). Maybe some interaction between Pt and PAn improves the stabilities of PAn.

Fig. 6 displays the CV curves of platinized XC-72 carbon and of different PAn–C composite modified electrodes in a 1.0 mol/L methanol + 1.0 mol/L H$_2$SO$_4$ medium. It demonstrates that more carbon in composite will increase the methanol oxidation peak current, because the conductivity of carbon is higher than that of PAn. The oxidation peak potentials of methanol with the four catalysts are 0.79 V, 0.73 V, 0.72 V, and
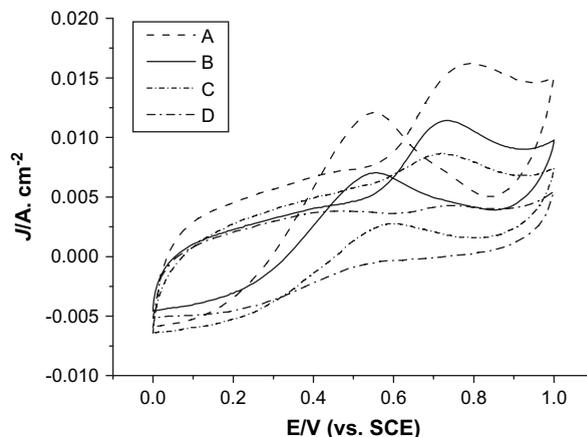

Fig. 6. CV curves of different platinized composite carriers in 1.0 mol/L H$_2$SO$_4$ + 1.0 mol/L CH$_3$OH media. A: 0.125:1 PAn–C; B: 0.25:1 PAn–C; C: 0.5:1 PAn–C; D: 0.75:1 PAn–C.
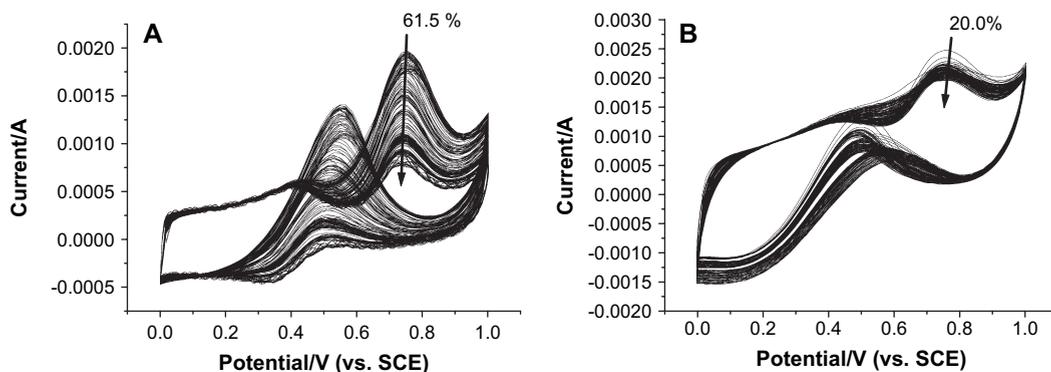
Fig. 7. CV curves for platinized-carrier-modified electrodes in 1.0 mol/L H_2SO_4 + 1.0 mol/L CH_3OH medium. A: Pt/C, for 200 circles; B: Pt/0.25:1 PAn–C, for 200 circles.

0.75 V. When PAn:C = 0.25:1 or 0.5:1, they are the most negative. The onset oxidation potentials of methanol oxidation with the four kinds of catalysts are 0.54 V, 0.49 V, 0.53 V, and 0.65 V. That of composite with PAn:C = 0.25:1 is the most negative too. It is concluded that the catalytic activity of Pt/0.25:1 PAn–C is better than that of the others.

After 200 CV cycles, the methanol oxidation current declines by 61.5% on the Pt/C catalyst, but it only declines by 20% on Pt/0.25:1 PAn–C composite catalyst because of the CO poisoning intermediate product (Fig. 7). The anti-poisoning ability of Pt/0.25:1 PAn–C is better than that of Pt/C about three times. The existence of PAn helps water absorption on the catalyst, and formation of an active oxycompound Pt–OH$_{ads}$, which will promote CO oxidation to CO_2. Furthermore, the better dispersity of Pt particles on composite will reduce the absorption points of the toxic intermediate [19]. PAn also accelerates the Langmuir absorption behavior of methanol [20]. In addition it is known that methanol absorption is the lowest step for its oxidation on Pt. So faster absorption is in favor of methanol oxidation. All the synergistic effects offer special properties to the composite catalyst. We can consider that some synergistic catalysis between PAn–C composite and Pt catalyst promotes the catalytic ability and enhances the anti-poisoning ability of the PAn compound catayst, but it needs a more detailed study to elucidate their mechanism of action.

Acknowledgements

References

[1] V.S. Bagotzky, Y.B. Vassilyev, Electrochim. Acta 12 (1967) 1323.
[2] S.L. Gojkovic, T.R. Vidakovic, Electrochim. Acta 47 (2001) 633.
[3] J.M. Leger, J. Appl. Electrochem. 31 (2001) 767.
[4] Y.T. Xu, Y.Y. He, L.Z. Dai, J.Y. Gal, H.H. Wu, Chem. J. chem. Univ. 24 (2003) 1915.
[5] A. Lima, F. Hahn, J.M. Leger, Russ. J. Electrochem. 40 (2004) 326.
[6] A.M.C. Luna, J. Appl. Electrochem. 30 (2000) 1137.
[7] H. Shioyama, Y. Yamada, A. Ueda, T. Kobayashi, Carbon 41 (2003) 607.
[8] Y.H. Lin, X.L. Cui, C. Yen, C.M. Wai, J. Phys. Chem. B 109 (2005) 14410.
[9] T. Kessler, A.M.C. Luna, J. Solid State Electrochem. 7 (2003) 593.
[10] J. Niessen, U. Schroder, M. Rosenbaum, F. Scholz, Electrochem. Communi. 6 (2004) 571.
[11] L. Niu, Q.H. Li, F.H. Wei, S.X. Wu, P.P. Liu, X.L. Cao, J. Electroanal. Chem. 578 (2005) 331.
[12] J.C. Park, J.S. Kim, D.H. Jung, Macromol. Res. 10 (2002) 181.
[13] B. Rajesh, K.R. Thampi, J.-M. Bonard, H.J. Mathieu, N. Xanthopoulos, B. Viswanathan, J. Power Sources 141 (2005) 35.
[14] J.M. Kinyanjui, N.R. Wijeratne, J. Hanks, D.W. Hatchett, Electrochim. Acta 51 (2006) 2825.
[15] G. Wu, L. Li, J.H. Li, B.Q. Xu, Carbon 43 (2005) 2579.
[16] G. Wu, L. Li, J.H. Li, B.Q. Xu, J. Power Sources 155 (2006) 118.
[17] M.C. Roman-Martinez, D. Cazorla-Amoros, Carbon 33 (1995) 3.
[18] S. Tawde, D. Mukesh, J.V. Yakhmi, Synth. Met. 125 (2001) 401.
[19] W.T. Napporn, H. Laborde, J.-M. Léger, C. Lamy, J. Electroanal. Chem. 404 (1996) 153.
[20] K.R. Prasad, J. Power Sources 103 (2002) 300.